DESCRIPTION AND PRELIMINARY VALIDATION OF A MODEL FOR NATURAL CONVECTION HEAT AND AIR TRANSPORT IN PASSIVE SOLAR BUILDINGS

G. F. Jones and J. D. Balcomb
Los Alamos National Laboratory
Los Alamos, New Mexico 87545

ABSTRACT

We have proposed a transient, quasi-two-dimensional, numerical model for interzone heat flow and airflow in passive solar buildings [1]. The paths for heat flow and airflow are through connecting apertures such as doorways, hallways, and stairways. The model includes the major features that influence interzone convection as determined from the results of our flow visualization tests, and temperature and airflow measurements taken in more than a dozen passive solar buildings. The model includes laminar and turbulent quasi-steady boundary-layer equations at vertical heated or cooled walls which are coupled to a one-dimensional core model for each zone. The cores in each zone exchange air and energy through the aperture which is modelled by a Bernoulli equation. Preliminary results from the model are in general agreement with data obtained in full-scale buildings and laboratory experiments. The model predicts room-core temperature stratification of about 2°C/m (1.1°F/ft) and maximum aperture velocities of 0.08 m/s (15 ft/min.) for a room-to-room temperature difference of 1°F.

1. INTRODUCTION

Natural convection plays a major role in the transport of heat in most passive solar buildings, especially those that employ sunspaces or atria as the solar heat collection element. The convective exchange typically involves normal building architectural elements (referred to as apertures in this paper) such as rooms, doorways, hallways, stairways, and interior windows.

As part of a multi-faceted program to gain greater understanding of this complex problem, Los Alamos has taken temperature, velocity, and solar radiation data in more than a dozen full-scale buildings having a variety of different designs [2-4]. Flow visualization studies have also been performed. We have found that large naturally driven heat and air transfer occurs with modest differences in temperature between rooms. For example, sunspace airflow and heat transfer rates of 0.222 to 1.06 m^3/s (470 to 2240 cfm) and 0.63 to 6.2 kW (2140 to 21,100 Btu/h) respectively have been observed near mid-day in moderate-sized residential buildings for temperature differences ranging from 1.7 to 5.6°C (3 to 10°F). In addition, we also observe significant room-core stratification [0.91 to 2.19°C/m (0.5 to 1.2°F/ft)] during periods of strong solar heating.

Building geometry and aperture flow areas have a major influence on thermal performance and comfort, and a simulation model is a necessary tool. This requires development of models for each convection process (element models), and a combination of the elements into a building simulation. Some element models are already well established. For example, aperture flows have been shown to agree quite well with predictions of a simple orifice model (sometimes referred to as a "Bernoulli model") [2,4,5], and several boundary-layer analyses have also been reported for natural convection on vertical and horizontal walls. In addition, there have been a considerable number of studies, both experimental and theoretical, to model the heat exchange in rectangular enclosures and some in two-room enclosures. But, full-scale buildings are much more complex, and existing analyses are too restricted to be of much quantitative use.

The model discussed in this paper is a first step to predict temperatures, airflows, and heat transfer in passive solar buildings without resorting to detailed numerical solutions. In the interest of simplicity, our approach to this model is to include approximate heat transfer from principal heat transfer surfaces, approximate airflow rates through apertures, and approximate local temperature distributions only in those locations where they are needed to address thermal comfort issues. At present, the model includes the effects that are common among most of the buildings

that we have monitored. As more data from a broader range of building designs become available, more elements may be added or the present elements may be adjusted to account for effects that are not currently treated.

2. GENERALIZATIONS BASED ON OBSERVATIONS AND DATA

We have constructed a composite diagram depicting airflow patterns found to be typical in most of the LANL full-scale passive building measurements (Fig. 1). Airflow patterns were determined by using either smoke, titanium tetrachloride vapors, or small helium-filled soap bubbles [6] as flow markers. The building shown in Fig. 1 is simplified and includes only two rooms connected by a lower and an upper aperture but still possesses all of the basic phenomena that we have observed. The south room is a double-glazed, solar-heated sunspace with a mass wall on its north side and a massive floor, and the north room is the living space with a north wall that loses heat to the outside and/or stores heat. The flow lines shown in Fig. 1 would occur on a winter day with bright sunshine.

Typically, the glazing in the sunspace operates about 5.6°C (10°F) warmer than the sunspace air when it is in direct sun. Referring to Fig. 1, vigorous boundary layer motion along the vertical glazing results from this large temperature difference, which entrains cool air from the core of the sunspace. We have measured velocities in the glazing boundary layers that range to about 0.46–0.61 m/s (18–24 in/s). Preliminary estimates show that the solar-heated glazing in the sunspace typically accounts for more than half of the heat flow and airflow from this space into the building during periods of strong solar heating—the remainder of it coming from the sunspace's warm north wall by weak boundary layer motion and warm floor. The inertia from this vigorous convective flow carries most of the involved air up into the space above the top of the glazing and above the upper edge of the upper aperture. There, the air mixes somewhat as it travels north and downward toward the upper aperture. The air in this mixed layer is nearly isothermal with a tendency for the temperature to be slightly cooler at the top of the layer from heat transfer to the usually massive roof structure (an unstable stratification that would tend to mix). The remaining air in the sunspace core is nearly motionless (away from the apertures) and is always stratified [0.91–2.19°C/m (0.5 to 1.2°F/ft)] during periods of significant interzone convection through the apertures. The evidence strongly suggests that convective exchange and stratification are intimately linked, although the dynamics of the processes that occur are not yet completely clear.

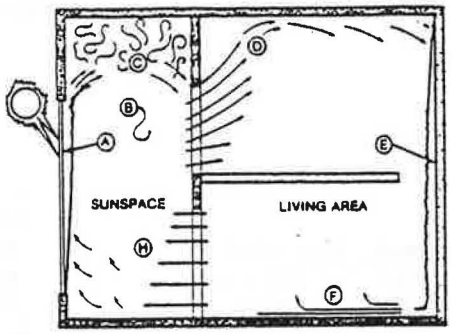

Fig. 1. Sketch of observed airflow in a strongly solar-heated passive building (elevation cross-sectional view). Letters designate the following effects:
(A) strong upward boundary-layer flow on the glazing;
(B) weak boundary-layer flows from other warm vertical walls in sunspace;
(C) mixed pool of air above glazing and upper aperture;
(D) warm air passing through the aperture and rising to its own density (or temperature) level;
(E) downward boundary-layer flow on the cool north wall;
(F) cool air stream returning to sunspace;
(G) airflow distribution through lower aperture into the sunspace;
(H) airflow rising as it passes over warm sunspace floor.

For the situation in Fig. 1, the airflow through each aperture is depicted as one way although an aperture often passes flow in both directions simultaneously. Typically, the velocity distribution across the aperture varies nearly as the square root of the distance from an imaginary plane of zero room-to-room pressure difference (neutral plane). This result is expected from a Bernoulli equation written for an aperture connecting two unstratified rooms [7] as the aperture velocity varies as the square root of the room-to-room pressure difference and, from hydrostatics, the pressure in each room is linear in height. However, even for the measurable room-core stratification described above, the agreement between airflow data and Bernoulli model predictions is surprisingly good. For the case of a single aperture dividing two rooms, the location of the neutral surface shifts to approximately the aperture midheight as it must do to permit two-way aperture airflow and to balance the flows.

As the warm air passes through the upper aperture and into the cooler north room, it typically rises, seeking its own density level. If no match is found, it travels very rapidly to the ceiling and flows toward the north wall. Here, the process described above occurs in reverse fashion where the cool boundary layer that forms on the north wall entrains the warmed flow from the cool-room core and ejects cool air at the floor level. The cool room is stratified in a manner similar to that of the sunspace.

As the cool stream of air enters the sunspace at the floor level, it passes over the sunlit floor and becomes warmer as it approaches the glazing. In some cases, we have noted this flow to rise into the sunspace core and not become entrained in the glazing boundary layer. In those regions of the sunspace floor that are not exposed to the return airflow from the cool room, no plume motion has been detected during the hours over which air and energy flows from the sunspace are large.

A more detailed description of the effects observed in the passive buildings that we have monitored is presented by Balcomb [8].

3.1 DESCRIPTION OF MODEL

Discussion of Elements and Their Interaction

Based on our flow visualization studies and data obtained for full-scale buildings, we have constructed the building-convection model from three basic elements (see Fig. 2): (1) boundary-layer flow and heat transfer at vertical heated or cooled surfaces in the building; (2) inviscid orifice flow and heat transfer through apertures; and (3) vertical and horizontal core flow and vertical temperature variation in each of the room cores.

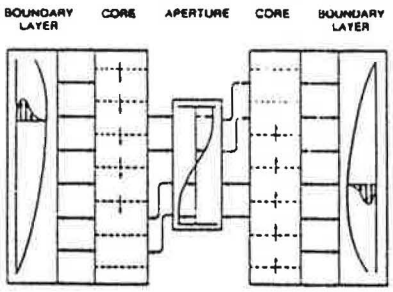

Fig. 2. Schematic diagram of proposed building-convection model depicting interaction among the elements.

The evidence of boundary-layer behavior on vertical heat transfer surfaces in buildings has been discussed earlier and its existence is consistent with results from all past studies of high Raleigh number convection in enclosures. The core model assumes horizontal isotherms in each zone which is in close agreement with our data for all building types, as well as with the results of others for high Rayleigh numbers. Heat transfer or subsequent air motion arising from heated or cooled horizontal surfaces are not included in the present version of the model. In addition, the present version of the model treats only two rooms connected by a single aperture or multiple apertures. In the rooms, only the end walls participate in the heat transfer (heating at the end wall in the south room and cooling at the end wall in the north room) and all other surfaces are insulated. The method however can be extended to multiple rooms having any number of vertical heat transfer surfaces and apertures. The effect of distributed building mass on convection processes is ignored for now.

Referring to Fig. 2, the interaction between the model elements is as follows: The boundary layers (which act as heat and air pumps) entrain or eject air from/to each of the cores. This process is controlled by the rate of growth or decay of the boundary-layer thickness (entraining when the boundary-layer thickens and ejecting when the boundary layer thins). The ejected or entrained airflow from the boundary layer feeds the core and causes a slow vertical core-air motion. In turn, the cores exchange air and heat through the apertures—a process that is controlled by the temperature distributions in each of the cores. In this way, the cores act to couple the heat transfer and airflows originating at the interior surfaces in one room to those occurring in an adjacent room through the connecting apertures. For a properly designed building, this coupling will exist without causing excessively high temperature differences among the cores so that the building remains comfortable.

The proposed model differs from existing nodal-network models in two ways. Firstly, nodal-network models utilize heat transfer coefficients between the walls and the room air; whereas, the proposed model does not. The coefficients which depend on such variables as geometry, thermal boundary conditions, and degree of stratification are usually not available. The proposed model takes account of these variables in determining the heat transport. Secondly, large nodal-network models do not include multiple vertical zones (i.e., no account for stratification); the proposed model

includes this as a major feature because of the strong effect of stratification on the heat transfer and thermal comfort. The proposed model provides more detailed information than these methods, namely, the stratification temperature profiles in each room. On the other hand, the proposed model provides less information than existing finite difference codes, because the enclosure has been replaced by boundary layer, core, and aperture models which involve a number of approximations. However, the additional detail given by the finite difference methods is not required for determining thermal performance, and the savings in computing time should be significant.

3.2 Description of Equations

The equations governing building temperature and airflow distributions that are used in the model are complicated and are not presented here for brevity. Because they are available in sufficient detail elsewhere [1], only a brief description of them is given.

Basically, the equations for the model are momentum, mass, and energy conservation for the boundary layers, mass and energy conservation for the cores, and an energy (orifice) equation for the apertures. The boundary layers and the aperture flows are treated as quasi-steady; only the core equations retain the time derivatives (estimates of time constants for the establishment of flows in these three elements show this to be an accurate assumption for conditions typical of buildings.)

The boundary-layer equations are written in integral form and with the usual procedure, they are reduced to two equations—one for the bondary-layer thickness and one for the boundary-layer velocity. Upon solution, air entrainment and heat transfer estimates are obtained directly from these two variables. The two equations can accommodate laminar, turbulent, or transition boundary-layer flow and a wide range of realistic thermal boundary conditions from isothermal to constant heat flux and any combination of the two.

Each core is divided into horizontal cells of small thickness and transient mass and energy conservation equations for the core are written for each cell. When solved, the equations provide estimates of core vertical airflow rates and vertical temperature distributions.

Aperture flows are driven by pressure differences tht arise from different temperatures in each room. Hydrostatic pressure distributions are first obtained by integrating the density (or reciprocal temperature) profiles over the room height. With these, an energy equation (often referred to as a "Bernoulli" or "orifice" equation) can then be solved for aperture velocity distributions. The airflow associated with this velocity leaves the core perpendicularly and passes through the aperture where it seeks its own density (or temperature) level. Once a match in temperature is found, the flow moves into the appropriate core cell without experiencing mixing during the process.

4.1 RESULTS AND DISCUSSION

Example Cases

We consider here a building with an adiabatic partition separating two air-filled rooms, each with height/length=2 and height/breadth=1. An aperture, centered in the partition, has a height and width of one-half and one-quarter of room height, respectively. The rooms are initially linearly stratified as shown in Fig. 3. At time=0 when the aperture is opened, flow is immediately established, and the computation predicts the evolution of the flow and the stratification temperature profiles with time. Two cases are considered. Case 1: All surfaces are adiabatic. Case 2: All surfaces are adiabatic except that the south wall is heated, and the north wall is cooled, both with constant heat flux. For simplicity we assume that the boundary layers are turbulent. For both cases the time step taken was about 2.5s and 21 core cells were used. For case 2, the rate of wall heating (by solar absorption in glazing) is 31.5 W/m^2 (10 Btu/h ft^2) and the room height is 2.4 m (8 ft).

The results for Case 1 are shown in Figs. 3-5. The temperature at the bottom of the warm room decreases in the expected manner (Fig. 3), as air from the cool room flows in through the bottom of the aperture (and conversely for the cool room). Vertical heat conduction in the cores is negligible here, with a time constant of 70 hours for H=2.4 m (8 ft). The net effect of the flow is to increase the stratification in each room, and ultimately the same nonlinear temperature profile is approached in each room. For H=2.4 m (8 ft), the three dimensionless times would correspond to 0.72, 2.15, and 4.47 minutes. The aperture flow distributions (Fig. 4) decay with time approximately exponentially with a time constant of about 2.1 minutes based on the total one-way flow.

The vertical core flow in the warm room (Fig. 5) is always zero for distance > 0.75, since flow from the warm room is

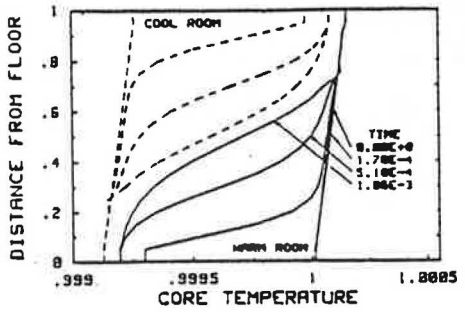

Fig. 3. Vertical temperature distributions in the warm and cool rooms after the opening of the aperture for Case 1 (adiabatic walls). Distance is scaled with room height and temperature with 1325 R. See text for times correspondence.

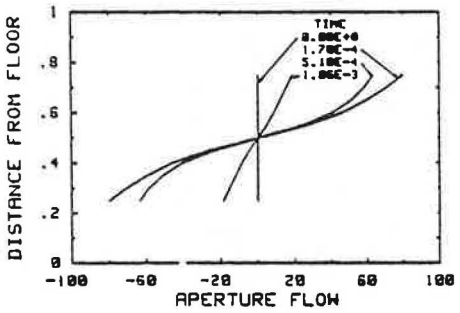

Fig. 4. Aperture flowrate distributions for Case 1. Distance is scaled with room height and flow with 5.7×10^{-3} m^3/s.

trapped above the aperture upper sill. The vertical flow distributions are quite different for the three times. At time=1.7×10^{-4}, the cold inflow drops directly to the floor of the warm room, since it is colder than the air at floor level. The lower half of the warm room received no horizontal flows from the aperture, and so the core flow remains constant in that range (a "slug flow"). From 0.5 < distance < 0.75, the vertical core flow drops to zero as the warm-room core delivers horizontal flow to the cold room via the aperture. For time=5.1×10^{-4}, only a portion of the cold inflow drops to the floor; the remainder enters the core at corresponding temperature levels. There still remains as region (0.2 < distance < 0.5) of "slug flow" since fluid from the cold room has no temperature correspondence in this range. At time=10.6×10^{-4}, there is no region of slug flow, and both the upper and lower regions of both rooms have become stagnant.

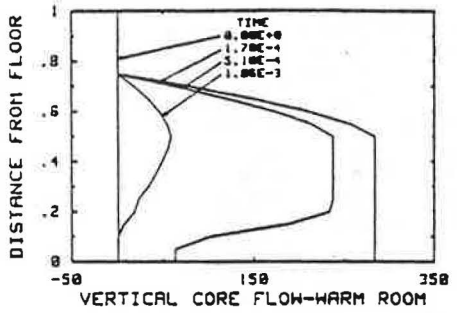

Fig. 5. Warm-room vertical flowrate distributions for Case 1. See Fig. 4 for scaling.

Now turning to Case 2 with end-wall heating and cooling, the warm room temperature distribution (Fig. 6) is quite different from Case 1 (Fig. 3). The warm room is hotter at the ceiling due to the rising warm boundary-layer flow. And it is colder at the floor, since the inflow from the cold room is colder due to the influence of the cooled-wall boundary layer. The net result is a substantial increase in stratification. The aperture flow (Fig. 7) drops only slightly, showing that the wall heat flux was almost sufficient to maintain the room temperature difference.

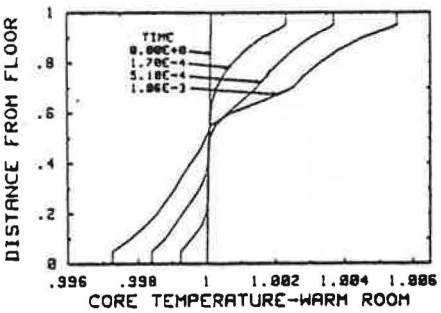

Fig. 6. Vertical temperature distributions in the warm room at three times after the opening of the aperture for Case 2 (end-wall heating and cooling). See Fig. 3 for scaling.

4.2 Preliminary Validation

In full-scale buildings, we have measured core-temperature gradients that range from 0.91 to 2.19°C/m (0.5 to 1.2°F/ft) during periods of strong solar heating. From the latest temperature profile shown in Fig. 6 (which is approaching steady state), we estimate the temperature gradient to be

about 2.4°C/m (1.3°F/ft)— in close agreement with the above range. For a room-core temperature difference of 0.56°C (1°F), the data obtained from full-scale buildings show a maximum aperture velocity of about 0.09 m/s (17 ft/min.). From Fig. 7, the maximum velocities range from 0.07 to 0.08 m/s (12.5 to 14.4 ft/min.) which again agrees with the data to within the expected accuracy of the model. The above comparisons of data and model predictions are, by no means, intended as a final validation. The validation process will be ongoing as additional effects are included in the model and as the data base for building convection increases. However, the good agreement does indicate that the model presently contains the principal features that influence natural convection heat transport in buildings during periods of significant solar heating.

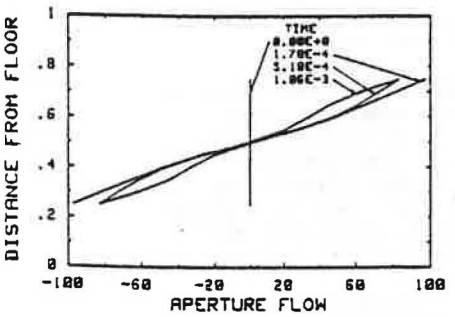

Fig. 7. Aperture flowrate distribution for Case 2. See Fig. 4 for scaling.

5. CONCLUSIONS

We have described a transient, two-dimensional model for interzone heat transfer in passive solar buildings. We have included in the current version of the model sufficient physics to predict transient room-core temperatures, heat transfer, and airflow through apertures. Results from the model are in general agreement with the data.

Generality of the model may be improved by including the effects of heat transfer at horizontal surfaces in the building—notably from cooled or warmed floors and ceilings. The convective heat transfer from these surfaces may account for a significant fraction of the energy flow from the sunspace during those hours where the glazing is not directly solar heated. In addition, a model for air mixing the core is needed to address air entrainment for a stream entering the core from boundary-layer ends and through apertures. Work is proceeding in these areas.

6. ACKNOWLEDGMENTS

This work was performed under the auspices of the US Department of Energy, Office of Solar Heat Technologies. The authors wish to acknowledge the significant contributions to this work made by Professor David R. Otis, and Kenjiro Yamaguchi and Mark White for their assistance in monitoring buildings. This paper was typed by Jan Sander and Loretta Duran.

7. REFERENCES

1. G. F. Jones, J. D. Balcomb, and D. R. Otis, "A Model for Thermally Driven Heat and Air Transport in Passive Solar Buildings," to be presented at the ASME Winter Annual Meeting, Miami Beach, Florida, November 17-22, 1985 (LA-UR-85-1519 (Rev.))

2. J. D. Balcomb and K. Yamaguchi, "Heat Distribution by Natural Convection," Proc. 8th Passive Solar Conf., Santa Fe, New Mexico, September 7-9, 1983 (LA-UR-83-1872).

3. J. D. Balcomb, G. F. Jones, and K. Yamaguchi, "Natural Air Motion and Stratification in Passive Buildings," Passive and Hybrid Solar Energy Update, Washington, D.C., September 5-7, 1984 (LA-UR-84-2650).

4. J. D. Balcomb and G. F. Jones, "Natural Air Motion in Passive Solar Buildings," Solar Buildings: Realities for Today, Trends for Tomorrow, Washington, D.C., March 18-20, 1985 (LA-UR-85-1045).

5. Hill, D., A. Kirkpatrick and P. Burns, "Interzonal Natural Convection Heat Transfer in a Passive Solar Building", To be presented at the 23rd AIChE/ASME National Heat Transfer Conference, Denver, Colorado, August, 1985.

6. M. D. White, A. T. Kirkpatrick, and C. B. Winn, "Flow Visualization of Interzonal Flow in Passive Solar Structures," Proc. ASME Solar Energy Division Meeting, Knoxville, Tennessee, March 25-28, 1985.

7. W. G. Brown and K. R. Solvason, "Natural Convection Through Rectangular Openings in Partitions, Part I: Vertical Partitions," Int. J. Heat and Mass Transfer 5, pp. 859-868, 1962.

8. J. D. Balcomb, "Heat Distribution by Natural Convection: Interim Report," Los Alamos National Laboratory report in preparation.